

Entropy-Driven Softening of Fluid Lipid Bilayers by Alamethicin

Georg Pabst,^{*,†} Sabine Danner,[†] Rudi Podgornik,^{‡,§,||} and John Katsaras^{⊥,♯,∇}

Institute of Biophysics and Nanosystems Research, Austrian Academy of Sciences, Schmiedlstrasse 6, A-8042 Graz, Austria, Laboratory of Physical and Structural Biology, NICHD, Building 9, Room 1E116, National Institutes of Health, Bethesda, Maryland 20892-0924, Faculty of Mathematics and Physics, University of Ljubljana, 1000 Ljubljana, Slovenia, Department of Theoretical Physics, Jožef Stefan Institute, 1000 Ljubljana, Slovenia, National Research Council, Canadian Neutron Beam Centre, Chalk River, Ontario K0J 1J0, Canada, Department of Physics, Brock University, 500 Glenridge Avenue, St. Catharines, Ontario L2S 3A1, Canada, and Department of Physics, Guelph–Waterloo Physics Institute and Biophysics Interdepartmental Group, University of Guelph, Guelph, Ontario N1G 2W1, Canada

Received May 31, 2007. In Final Form: August 10, 2007

Using dilatometry and small-angle X-ray diffraction, we have studied under bulk conditions the structural changes and elastic response of dioleoyl phosphatidylcholine bilayers to alamethicin. With increasing peptide concentration, we found a progressive thinning of the membrane. However, in contrast to previously published reports, this thinning exhibits exponential behavior. Furthermore, an increase in alamethicin content resulted in an increased lateral area per lipid and a swelling of the multibilayers which can be attributed to a decrease in the bilayer's bending rigidity by ~50%. At the same time, hydration and van der Waals forces remained unaffected by the presence of the peptide. Interestingly, all elastic and structural parameters followed the same exponential form found for the membrane thickness, implying a common underlying mechanism for all of these structural parameters. Our results can be understood by introducing an additional entropy term into the free-energy description of peptide incorporation, a term previously not considered. As a result, we have been able to reconcile recent controversies regarding the effect of peptides on membrane thinning.

1. Introduction

The rapid increase in the number of antibiotic-resistant bacterial strains has resulted in considerable efforts being expended in the search for novel antibiotics, particularly with regard to antimicrobial peptides (AMPs) which are intrinsic to the immune system and represent the first line of defense against invading pathogens.^{1–4} Among the most intriguing properties of AMPs are their nonspecific mode of action and their ability to discriminate between mammalian and bacterial cells, which are believed to be governed by a delicate interplay between electrostatic and hydrophobic interactions.^{5–9} The two commonly discussed molecular models of membrane disruption by AMPs are the so-called carpet¹⁰ and pore-formation mechanisms,¹¹ where

the latter distinguishes between barrel–stave and toroidal (wormhole) pores. Using neutron diffraction, Huang and co-workers¹² have demonstrated the existence of both types of pores in membranes. However, given the complex lipid composition of natural membranes, one can imagine other membrane disruption mechanisms (e.g., peptide-induced lipid segregation or a shift in lipid phase-transition temperatures).^{4,13} For example, it has recently been shown that LL-37 may either induce the formation of disklike micelles in phosphatidylcholines (PCs) or lead to the formation of a quasi-interdigitated phase in phosphatidylglycerols (PGs).¹⁴ Nevertheless, even if one overlooks the remaining ambiguities concerning the molecular mode of AMPs, from a physicochemical point of view these systems still present many challenging issues.

One issue is the mutual dependence of membrane and peptide properties. Several theoretical studies have looked at the influence of proteins perturbing lipid bilayers.^{15–23} According to elasticity theory, a single peptide adsorbed to the lipid bilayer creates a local deformation that propagates over a given length scale, which depends on the local hydrocarbon chain length, the bending rigidity K_C , and the area stretch modulus K_A .²⁰ Oriented circular

* To whom correspondence should be addressed. Tel: 43 316 4120 342. Fax: 43 316 4120 390. E-mail: georg.pabst@oeaw.ac.at.

† Austrian Academy of Sciences.

‡ National Institutes of Health.

§ University of Ljubljana.

|| Jožef Stefan Institute.

⊥ National Research Council.

♯ Brock University.

∇ University of Guelph.

(1) Boman, H. G. *Cell* **1991**, *65*, 205.

(2) Ganz, T. *Science* **1999**, *286*, 420.

(3) Zasloff, M. *Nature* **2002**, *415*, 389.

(4) Lohner, K.; Blondelle, S. E. *Comb. Chem. High Throughput Screening* **2005**, *8*, 241.

(5) Epanand, R. M.; Vogel, H. J. *Biochim. Biophys. Acta* **1999**, *1462*, 11.

(6) Lohner, K.; Prenner, E. J. *Biochim. Biophys. Acta* **1999**, *1462*, 141.

(7) Lohner, K. In *Development of Novel Antimicrobial Agents: Emerging Strategies*; Lohner, K., Ed.; Horizon Scientific Press: Wymondham, Norfolk, England, 2001; p 149.

(8) Dathe, M.; Meyer, J.; Beyermann, M.; Maul, B.; Hoischen, C.; Bienert, M. *Biochim. Biophys. Acta* **2002**, *1558*, 171.

(9) Zwegytick, D.; Pabst, G.; Abuja, P. M.; Jilek, A.; Blondelle, S. E.; Andra, J.; Jerala, R.; Monreal, D.; Martinez, d. T.; Lohner, K. *Biochim. Biophys. Acta* **2006**, *1758*, 1426.

(10) Oren, Z.; Shai, Y. In *Development of Novel Antimicrobial Agents: Emerging Strategies*; Lohner, K., Ed.; Horizon Scientific Press: Wymondham, Norfolk, England, 2001; p 183.

(11) Matsuzaki, K. In *Development of Novel Antimicrobial Agents: Emerging Strategies*; Lohner, K., Ed.; Horizon Scientific Press: Wymondham, Norfolk, England, 2001; p 167.

(12) Huang, H. W. *Biochim. Biophys. Acta* **2006**, *1758*, 1292.

(13) Pabst, G.; Danner, S.; Karmakar, S.; Deutsch, G.; Raghunathan, V. A. *Biophys. J.* **2007**, *93*, 513.

(14) Sevcsik, E.; Pabst, G.; Jilek, A.; Lohner, K. *Biochim. Biophys. Acta*, in press.

(15) Mouritsen, O. G.; Bloom, M. *Biophys. J.* **1984**, *46*, 141.

(16) Dan, N.; Pincus, P.; Safran, S. A. *Langmuir* **1993**, *9*, 2768.

(17) Dan, N.; Berman, A.; Pincus, P.; Safran, S. A. *J. Phys. II (France)* **1994**, *4*, 1713.

(18) Huang, H. W. *J. Phys. II (France)* **1995**, *5*, 1427.

(19) Dan, N.; Safran, S. A. *Biophys. J.* **1998**, *75*, 1410.

(20) May, S. *Curr. Opin. Colloid Interface Sci.* **2000**, *5*, 244.

(21) Zuckermann, M. J.; Heimburg, T. *Biophys. J.* **2001**, *81*, 2458.

(22) Zemel, A.; Ben Shaul, A.; May, S. *Biophys. J.* **2004**, *86*, 3607.

(23) Zemel, A.; Ben Shaul, A.; May, S. *Eur. Biophys. J.* **2005**, *34*, 230.

dichroism experiments, pioneered by Huang et al., have shown that surface-adsorbed peptides, or so-called S-state peptides, occur at very low concentrations.¹² However, a recent diffraction study found that α -helical peptides have to be, at a minimum, in the dimeric form in order to perturb the membrane.²⁴ Hence, the self-association of surface-adsorbed AMPs is believed to be a precursor to peptide insertion (I state) and subsequent pore formation²³ which takes place when the peptide/lipid (P/L) molecular ratio is above a certain threshold P/L^* .¹² Peptide oligomerization and pore formation require the penalties imposed by the entropy and repulsion of similarly charged proteins to be overcome. Besides the common theoretical agreement that protein interactions are mediated by bilayer properties,^{16–18,25} there are currently three models that deal with the S- to I-state transition. According to Zuckermann and Heimburg,²¹ surface-adsorbed peptides can be treated as a 2D gas exerting a lateral pressure, which, at elevated concentrations, results in the peptide inserting into the membrane. Alternatively, Huang and co-workers considered the possibility that with increasing peptide concentration the membrane deforms, driving the transition into the I state.^{12,18,26} Finally, a molecular-level model calculation suggests that lipid chains gain in conformational freedom when the peptide inserts itself into the membrane.²³

With respect to the global elastic response of the lipid bilayer to peptide inclusions, the consensus seems to be that there is an overall linear thinning of the lipid bilayer when $P/L < P/L^*$ by a few ångströms and a constant membrane thickness d_B for $P/L > P/L^*$.¹² Little is known about the bilayer's overall elastic response in terms of its bending rigidity K_C and bilayer interactions. For example, a theoretical report based on elastic continuum theory claims that K_C should increase as the protein is dissolved in the lipid bilayer.²⁷ However, a different theoretical treatment, which includes the effects of molecular lateral diffusion, shows that membrane rigidity may also be reduced.²⁸ Nevertheless, despite the theoretical predictions, there have been few experimental reports. A membrane stiffening effect for distearoyl phosphatidylglycerol monolayers in the presence of the frog skin peptide PGLa was surmised from X-ray grazing incidence diffraction studies, while being implicated in the softening of distearoyl phosphatidylcholine.²⁹ In contrast, X-ray reflectometry studies of solid-supported charged and uncharged multibilayers in the presence of magainin 2 and at relative humidities (RH) slightly below 100% showed increased bending fluctuations, pointing to a reduction in K_C .^{30,31} To the best of our knowledge, no direct measurement of the bending rigidity in the presence of a protein or peptide has been reported. Moreover, lipid monolayers may not be equivalent in terms of the bilayer's elastic response, and bilayers may behave differently in the presence of peptides under fully hydrated conditions. Recently, finite size effects have been reported for very thin lipid films,^{32,33} possibly affecting the results if highly aligned bilayers with less than ~ 10 layers are studied. An additional motivating factor for the present studies was drawn from a recent X-ray reflectometry study of

various model membranes³¹ which has challenged the universality of the membrane thinning effect reported by Huang et al.¹²

We have performed dilatometric and small-angle X-ray diffraction studies on osmotically stressed dioleoyl phosphatidylcholine (DOPC) multibilayers containing various concentrations of alamethicin. Alamethicin³⁴ is a well-known ionophore (see, for example, refs 35 and 36), and both DOPC and alamethicin have been extensively studied. Our experimental conditions differ, however, from the previous diffraction studies by Huang et al.¹² and Salditt et al.^{30,31} in that we studied the systems under bulk conditions (i.e., fully hydrated liposomal dispersions) eliminating any possible complications due to less than fully hydrated bilayers. Here we provide evidence for the distinct softening of lipid bilayers in the presence of alamethicin, whereas other bilayer interactions remained largely unaffected. We also clearly observed a thinning of the membrane. However, in contrast to the studies by Huang and co-workers,¹² the thinning was exponential. Interestingly, all other studied parameters such as bilayer separation, area per lipid, and bending rigidity also followed the same exponential form with increasing peptide concentration. We were able to describe these findings qualitatively by taking into account an additional entropic contribution to the free energy of peptide insertion. This allowed us to reconcile the disparate results reported by Huang et al. and Salditt et al.^{12,31}

2. Materials and Methods

2.1. Sample Preparation. Dry powder of 1,2-dioleoyl-*sn*-glycero-3-phosphatidylcholine (DOPC) was purchased from Avanti Polar Lipids (Alabaster, AL). Alamethicin (from the fungus *Trichoderma viride*³⁴), polyethylene glycol (PEG) (MW $\approx 20\,000$), chloroform, and methanol (p.A. grade) were obtained from Sigma-Aldrich (St. Louis, MO). Both the lipid (claimed purity $>99\%$) and peptide (claimed purity $>90\%$) were used without further purification.

Stock lipid and alamethicin solutions were prepared by dissolving lipid and peptide powders in chloroform/methanol (2/1 v/v). Appropriate amounts of the stock solutions were mixed to obtain the desired L/P ratio and subsequently dried under a gentle stream of N_2 . The glass vials containing the lipid films were then placed under vacuum for 8 h to remove the remaining solvent. Dry lipid/peptide films were hydrated in 18 M Ω /cm water (UHQ PS,USF Elga, Wycombe, U.K.) at room temperature for 4 h, while being intermittently vortex mixed. This method of preparation yielded multilamellar vesicles (MLVs), as verified by X-ray diffraction (see below). The total lipid concentration was 50 mg/mL for X-ray experiments and 5 mg/mL for dilatometry measurements.

Osmotically stressed samples were centrifuged at 6000 rpm for 8 min (Sigma 3K18, Sigma Laborzentrifugen, Osterode am Harz, Germany). The supernatant was then removed, weighed, and replaced by the appropriate wt % PEG solutions. Samples were subsequently equilibrated at room temperature for 2 days. Osmotic pressures were determined using the data published on http://www.brocku.ca/researchers/peter_rand/osmotic/osfile.html, taking into account the dilution of the PEG solution by the excess water in the lipid pellet. Thin layer chromatography, prior to and after experimentation, showed no signs of sample degradation.

2.2. Dilatometry. The suitability of dilatometry to determine lipid/peptide interactions has been previously demonstrated.³⁷ Densities of fully hydrated DOPC MLVs in the presence of alamethicin were obtained using a DSA 5000 dilatometer (Anton Paar, Graz, Austria), which consists of a vibrating U-shaped borsillica glass tube containing the lipid dispersion and a vibrating reference glass rod.^{38,39} Temperature control was provided by a Peltier circuit with a claimed density measurement accuracy of 10^{-6} g/mL. Sedimentation, or

(24) Hristova, K.; Dempsey, C. E.; White, S. H. *Biophys. J.* **2001**, *80*, 801.

(25) Lague, P.; Zuckermann, M. J.; Roux, B. *Biophys. J.* **2001**, *81*, 276.

(26) Lee, M. T.; Chen, F. Y.; Huang, H. W. *Biochemistry* **2004**, *43*, 3590.

(27) Chen, C. M. *Physica A* **2000**, *281*, 41.

(28) Divet, F.; Danker, G.; Misbah, C. *Phys. Rev. E* **2005**, *72*.

(29) Kononov, O.; O'Flaherty, S. M.; Saint-Martin, E.; Deutsch, G.; Sevcik, E.; Lohner, K. *Physica B* **2005**, *357*, 185.

(30) Salditt, T. *Curr. Opin. Struct. Biol.* **2003**, *13*, 467.

(31) Li, C.; Salditt, T. *Biophys. J.* **2006**, *91*, 3285.

(32) Harroun, T. A.; Raghunathan, V. A.; Pencer, J.; Nieh, M. P.; Katsaras, J. *Phys. Rev. E* **2004**, *70*.

(33) Harroun, T. A.; Koslowsky, M.; Nieh, M. P.; Raghunathan, V. A.; Katsaras, J. *Eur. Phys. J. E* **2004**, *13*, 359.

(34) Martin, D. R.; Williams, R. J. *Biochem. J.* **1976**, *153*, 181.

(35) Aguilera, V. M.; Bezrukov, S. M. *Eur. Biophys. J.* **2001**, *30*, 233.

(36) Bezrukov, S. M.; Vodyanov, I. *Biophys. J.* **1997**, *73*, 2456.

(37) Posch, M.; Rakusch, U.; Mollay, C.; Lagner, P. *J. Biol. Chem.* **1983**, *258*, 1761.

floatation sample effects were found to be negligible as determined by repeating the measurements with freshly prepared samples.

The apparent partial specific volume of the dispersion was calculated from

$$\varphi_V = \frac{1}{\tilde{\rho}_0} \left(1 - \frac{\tilde{\rho} - \tilde{\rho}_0}{c} \right) \quad (1)$$

where $\tilde{\rho}_0$ and $\tilde{\rho}$ are the measured densities of water and the lipid dispersion, respectively, and c is the total lipid/peptide concentration. Following Greenwood et al.,⁴⁰ we determined the partial volumes of DOPC (V_L) and alamethicin (V_P) by first calculating the volume per molecule using

$$V = \frac{\varphi_V}{N_A} [x_P M_P + (1 - x_P) M_L] \quad (2)$$

where N_A is Avogadro's number, M_P and M_L are the molecular weights of the peptide and the lipid, respectively, and $x_P = N_P/(N_P + N_L)$, where N_P and N_L are the numbers of peptide and lipid molecules, respectively. The partial molecular volumes are then given by the expression⁴⁰

$$V_P = V + (1 - x_P) \frac{dV}{dx_P} \text{ and } V_L = V - x_P \frac{dV}{dx_P} \quad (3)$$

2.3. Small-Angle X-ray Diffraction (SAXD). SAXD measurements were performed using a SWAX camera (Hecus X-ray Systems, Graz, Austria) mounted on a sealed tube X-ray generator (Seifert, Ahrensburg, Germany) operating at 2 kW. Cu K α radiation ($\lambda = 1.542 \text{ \AA}$) was selected using a Ni filter in combination with a pulse-height discriminator; the X-ray beam size was set to $0.5 \text{ mm} \times 34 \text{ mm}$. Samples were transferred into 1 mm thin-walled quartz glass capillaries, and prior to each measurement, they were equilibrated at $25 \text{ }^\circ\text{C}$ for 10 min using a programmable Peltier unit. The scattering intensity was recorded using a linear position-sensitive detector (Hecus X-ray Systems, Graz, Austria) for wave vectors ($q = 4\pi \sin(\theta)/\lambda$, where θ is half the scattering angle) between 10^{-3} and 1 \AA^{-1} . An exposure time of 7200 s was chosen in order to obtain good counting statistics at higher q values. Detector channel numbers were converted to wave vectors using a silver stearate standard.

Diffraction patterns were corrected for background scattering originating from the capillary and polymer solution, or water, and were further analyzed using GAP (global analysis program), a program based on a previously developed global data analysis technique. (For a review, see ref 41.) In brief, the scattering intensity from MLVs is modeled as

$$I(q) = \frac{S(q)|F(q)|^2}{q^2} \quad (4)$$

where $S(q)$ is the structure factor determined from Caillé theory,^{42,43} and $F(q)$ is the form factor obtained from fitting the electron density profile.⁴⁴ From the fit parameters we determined the membrane thickness

$$d_B = 2(z_H + 2\sigma_H) \quad (5)$$

where z_H and σ_H are the Gaussian's position and width, respectively, describing the electron-dense part of the electron density profile. The lateral area per lipid is given by⁴²

$$A_L = \frac{V_L - V_H}{d_C} \quad (6)$$

where the headgroup ($V_H = 319 \text{ \AA}^3$ for PCs⁴⁵) and lipid volumes (V_L) were obtained from dilatometry. (See above.) The hydrocarbon chain length is given by $d_C = z_H - 4 \text{ \AA}$.

The fluctuation, or so-called Caillé parameter,⁴² also obtained from the global X-ray data analysis, is given as follows

$$\eta = \frac{\pi k_B T}{2d^2 \sqrt{BK_C}} \quad (7)$$

η describes the power law decay of Bragg peaks and includes the Boltzmann constant (k_B), the temperature (T), the lamellar repeat distance (d) of the lipid bilayer stack, the bending rigidity (K_C) of a single bilayer, and the bulk modulus of compression (B) between two interacting membranes.^{46,47} To disentangle the two mechanical parameters, one can either perform surface diffraction experiments on highly aligned multibilayers,^{48,49} or use an osmotic pressure technique.^{50–52} We chose the latter.

We determined the bilayer interactions from MLVs under osmotic pressure Π using the relationship $\Pi = P_{vdW} + P_{hyd} + P_{fl}$,⁵⁰ where

$$P_{vdW} = -\frac{H}{6\pi} \left[\frac{1}{d_W^3} - \frac{2}{(d_W + d_B)^3} + \frac{1}{(d_W + 2d_B)^3} \right] \quad (8)$$

$$P_{hyd} = P_h \exp\left(\frac{-d_W}{\lambda_h}\right) \quad (9)$$

and

$$P_{fl} = \left(\frac{k_B T}{2\pi}\right)^2 \frac{A_{fl}}{K_C \lambda_{fl}} \exp\left(\frac{-d_W}{\lambda_{fl}}\right) \quad (10)$$

are the pressures corresponding to van der Waals (P_{vdW}), hydration (P_{hyd}), and fluctuation (P_{fl}) interactions, respectively. They involve the Hamaker coefficient H , the empirical scaling constants P_h and A_{fl} , and the decay lengths λ_h and λ_{fl} . Petrache et al.⁵⁰ determined A_{fl} and λ_{fl} by measuring Caillé parameter η (eq 7) as a function of Π and derived H , P_h , and λ_h from a least-square fit to $\Pi(d_W)$ data. This, however, requires high-resolution diffraction data and an accurate description of the shape of the Bragg peaks. In our case, the rectangular beam smeared the data, precluding the type of analysis carried out by Petrache et al., especially at high osmotic pressures where the diffuse signal, as a result of bending fluctuations, also happens to be weak. Only at $\Pi = 0$ were we able to obtain reliable values for η as a function of peptide content. (See also Figure 3E.) As a result of the limitations imposed on us by the instrument, we took a different approach to disentangling the two bilayer mechanical parameters.

First, we determined P_h and λ_h at high osmotic pressures ($\Pi > 12 \text{ atm}$), where bending fluctuations can be neglected and all data fall on a single straight line on a semilogarithmic plot of $\Pi(d_W)$. For van der Waals interactions, we used $H = 4.3 \text{ zJ}$, a value recently

(45) Sun, W. J.; Suter, R. M.; Knewton, M. A.; Worthington, C. R.; Tristram-Nagle, S.; Zhang, R.; Nagle, J. F. *Phys. Rev. E* **1994**, *49*, 4665.

(46) De Gennes, P. G.; Prost, J. *The Physics of Liquid Crystals*, 2nd ed.; Oxford University Press: Oxford, U.K., 1993.

(47) de Jeu, W. H.; Ostrovskii, B. I.; Shalaginov, A. N. *Rev. Mod. Phys.* **2003**, *75*, 181.

(48) Liu, Y.; Nagle, J. F. *Phys. Rev. E* **2004**, *69*, 040901.

(49) Salditt, T. *J. Phys.: Condens. Matter* **2005**, *17*, R287.

(50) Petrache, H. I.; Gouliavaev, N.; Tristram-Nagle, S.; Zhang, R. T.; Suter, R. M.; Nagle, J. F. *Phys. Rev. E* **1998**, *57*, 7014.

(51) Pabst, G.; Katsaras, J.; Raghunathan, V. A.; Rappolt, M. *Langmuir* **2003**, *19*, 1716.

(52) Petrache, H. I.; Tristram-Nagle, S.; Harries, D.; Kucerka, N.; Nagle, J. F.; Parsegian, V. A. *J. Lipid Res.* **2006**, *47*, 302.

(38) Kratky, O.; Leopold, H.; Stabinger, H. *Z. Angew. Phys.* **1969**, *27*, 273.

(39) Laggner P.; Stabinger, H. In *Colloid and Interface Science*; Kerker, M., Ed.; Academic Press: New York, 1976; p 91.

(40) Greenwood, A. I.; Tristram-Nagle, S.; Nagle, J. F. *Chem. Phys. Lipids* **2006**, *143*, 1.

(41) Pabst, G. *Biophys. Rev. Lett.* **2006**, *1*, 57.

(42) Caillé, A. C. R. *Acad. Sci. Paris B* **1972**, *274*, 891.

(43) Zhang, R.; Suter, R. M.; Nagle, J. F. *Phys. Rev. E* **1994**, *50*, 5047.

(44) Pabst, G.; Rappolt, M.; Amenitsch, H.; Laggner, P. *Phys. Rev. E* **2000**, *62*, 4000.

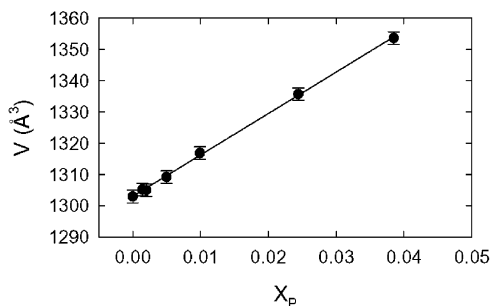


Figure 1. Molecular volumes of DOPC/alamethicin at 25 °C as a function of peptide concentration x_p . The solid line is a fit to the data from which the partial volumes of DOPC and alamethicin were obtained. (See the text.)

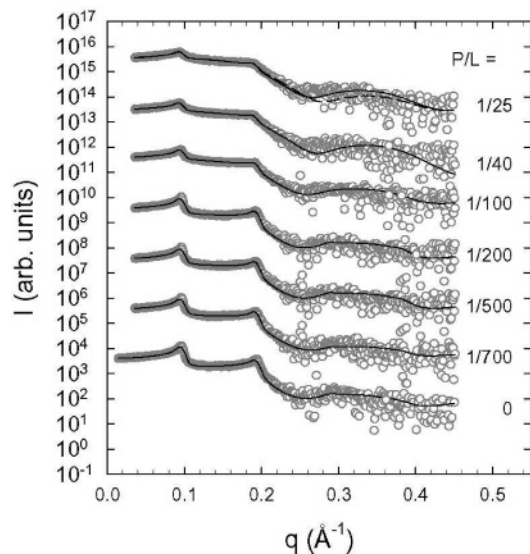


Figure 2. SAXD patterns of DOPC at 25 °C in the presence of alamethicin. For clarity, the patterns have been offset vertically. Numbers to the right of the data give the corresponding peptide/lipid molar ratio. Solid lines are fits to the data using the global analysis program.⁴¹ The dashed line shows the global fit for a membrane thickness of ≤ 0.3 Å. Increasing the membrane thickness by 0.3 Å leads to a fit that is difficult to distinguish visually from the best fit presented. However, its reduced χ^2 , reporting on the goodness of the fit,⁶⁰ is larger. All reported structural parameters correspond to the fit with the lowest χ^2 found.

calculated for lipid–water systems based on the full Lifshitz theory for multilamellar assemblies.⁵³ We then set $\lambda_{\Pi} = 2\lambda_h$ as predicted by an earlier theoretical consideration⁵⁴ of fluctuation-enhanced repulsive interactions, which scale as the square root of the bare interaction potential. A_{Π} was determined by fixing K_C to a reported value⁴⁸ and fitting over the full range of $\Pi(d_w)$. Finally, we fixed A_{Π} and left K_C and λ_h as the only adjustable parameters for bilayers containing alamethicin.

This analysis implicitly assumes that H and A_{Π} are not altered by the peptide. H depends on the dielectric spectrum of the bilayers, which to some extent will be affected by the presence of alamethicin. This change would in general tend toward a smaller Hamaker coefficient because the peptide would displace some of the low dielectric hydrocarbon chains with the larger dielectric polar moieties of the peptide, and the Hamaker coefficient depends on the difference between the dielectric constants. However, even at $P/L = 1/25$ the peptide concentration is still too low to cause a significant change. P_h and analogously A_{Π} , that contains P_h ,⁵⁰ strongly depend on the definition of membrane thickness. Osmotic pressure data at small

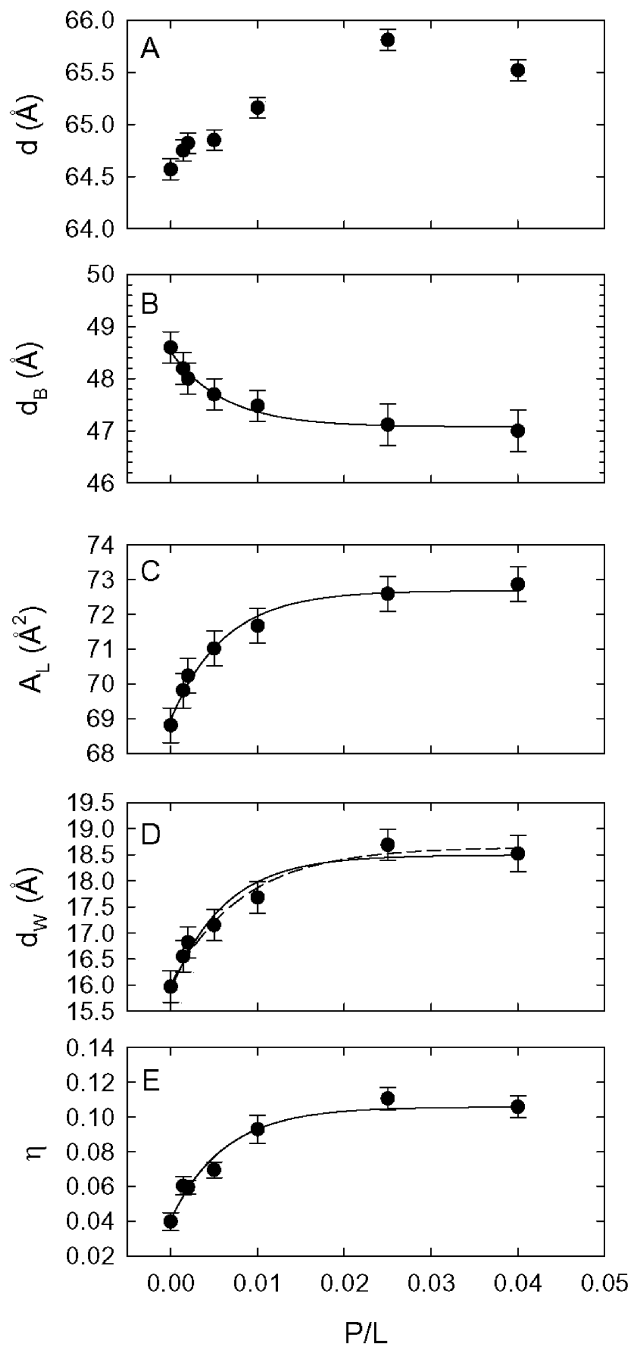


Figure 3. Structural parameters of DOPC as a function of alamethicin concentration. (A) Lamellar repeat distance, (B) membrane thickness, (C) lateral area per lipid, (D) bilayer separation, and (E) fluctuation parameter. The solid lines are exponential fits to the data with a decay constant of $P/L^* = 1/160$. The dashed line in panel D indicates a fit with $P/L^* = 1/120$.

intermembrane separations showed that P_h does not vary substantially with the P/L ratio. (See below.) The same would thus be true for A_{Π} , and this is the reason that we have kept A_{Π} constant in our analysis. This is also supported by Petrache et al.⁵⁵ who found A_{Π} to be independent of temperature in EggPC bilayers, despite a significant decrease of K_C . Nevertheless, we have verified this assumption by inducing a small change in A_{Π} . (See below.)

3. Results and Discussion

The partial molecular volumes of 25 °C DOPC bilayers containing alamethicin were determined as a function of ala-

(53) Podgornik, R.; French, R. H.; Parsegian, V. A. *J. Chem. Phys.* **2006**, *124*, 044709.

(54) Podgornik, R.; Parsegian, V. A. *Langmuir* **1992**, *8*, 557.

(55) Petrache, H. I.; Tristram-Nagle, S.; Nagle, J. F. *Chem. Phys. Lipids* **1998**, *95*, 83.

methicin concentration using dilatometry (Figure 1). The data were best fit by a straight line and are in contrast to the behavior exhibited by lipid/cholesterol mixtures, where V has been reported to decrease supposedly as a result of a condensing effect by cholesterol.⁴⁰ The present data imply that alamethicin increases membrane disorder, and the linear dependence of the molecular volume on peptide concentration shows that neither the lipid nor the peptide underwent a conformational change during the incorporation process. From the slope of V (eq 8), we determined V_L and V_P to be 1303 ± 1 and $2630 \pm 60 \text{ \AA}^3$, respectively. The DOPC result is in good agreement with previous data using a neutral flotation method.⁵⁶ With regard to the partial volume of the peptide V_P , we note that, to the best of our knowledge this is the first report of a peptide's partial molecular volume in the presence of a bilayer and can be compared to crystallographic data on alamethicin.⁵⁷ Using the program CRY SOL⁵⁸ we obtained an envelope volume of 2884 \AA^3 . This compares favorably to our value even though the program uses a 3 \AA hydration shell to cover the entire molecule, which is certainly not true for the portions of the peptide facing the lipid bilayer's hydrophobic interior. From this we conclude, in agreement with previous studies (see, for example, Bak et al.⁵⁹ and references therein), that the overall structure of alamethicin in DOPC bilayers closely resembles the crystallographic structure.

Figure 2 shows SAXS patterns of $25 \text{ }^\circ\text{C}$ stress-free DOPC dispersions at various alamethicin concentrations. Each pattern exhibits two lamellar diffraction orders. The asymmetric shape of the peak is due to geometrical smearing from using a rectangularly shaped X-ray beam, which is taken into account when fitting the data (solid lines in Figure 2). The data show small shifts in the peak positions to smaller q values as the amount of peptide is increased, indicating a small increase in the lamellar repeat distance d . This is unexpected because one would have predicted infinite swelling in a charged system—alamethicin carries a single negative charge—in the absence of counterions. The observation of finite bilayer separation, even at the highest alamethicin concentrations, signifies that electrostatic bilayer repulsion apparently plays, at best, a very small role and can thus be neglected when considering bilayer interactions. (See below.) More important than the changes in d as a function of increasing peptide concentration, is the decreased peak intensity and the concomitant increase in diffuse scattering, pointing to increased crystalline disorder as a result of bending fluctuations. Regardless of peptide concentration no scattering contribution from alamethicin was observed.

Figure 3 shows the results obtained when using global data analysis for the $\Pi = 0$ data presented in Figure 2. First, we deal with the parameters describing the overall membrane structure and then turn to the modulation of the bilayer interactions. Besides the slightly increasing d ($\sim 1 \text{ \AA}$) we find an almost 2 \AA decrease in membrane thickness (Figure 3B) over the range of alamethicin concentrations studied. Because d and d_B , as a function of P/L, exhibit opposite behavior, bilayer separation has to increase with increasing peptide concentration pointing to an increase in bending fluctuations (Figure 3D,E). We were also able to quantify the increase in the lateral area per lipid as a function of P/L. Our results confirm reports that as a function of increasing alamethicin concentration there is increasing bilayer disorder, previously expressed as membrane thinning.¹² Using $d_H = 10 \text{ \AA}$ for the PC

headgroup,⁶¹ our value for d_B of $47.0 \pm 0.3 \text{ \AA}$ at P/L = 1/25 yields a hydrophobic thickness of $2d_C = d_B - 2d_H = 27.0 \text{ \AA}$. This value is in good agreement with alamethicin/lipid studies performed by Huang and co-workers,¹² but is about $5\text{--}7 \text{ \AA}$ larger than alamethicin's estimated hydrophobic length.⁵⁹ Because at the highest peptide concentrations most of the alamethicin molecules are assumed to be in a transmembrane orientation, this implies that the DOPC bilayer distorts locally in order to match the bilayer and peptide hydrophobic regions.

For the most part, our results are in good overall agreement with previous work by Huang et al. However, we are in disagreement with a subtle yet important point made by Huang and co-workers.¹² In comparing membrane thicknesses we did not observe a linear decrease at low peptide concentrations and a constant d_B above P/L*. What we observed was a gradual decrease in d_B with P/L, which is well fit using an exponential decay (i.e., $d_B \propto \exp[-(P/L)/(P/L^*)]$). The decay constant P/L* = 1/160 is in reasonable agreement with P/L* \approx 1/200 reported from oriented circular dichroism.⁶² However, it is remarkable that an exponential form with the same decay constant also describes the lateral area per lipid, bilayer separation, and bending fluctuations data (Figure 3C–E). There is only a slight variation in P/L* if we allow it to adjust freely (Figure 3D). Hence, there is a strong implication for a common underlying mechanism that leads the various structural parameters to behave similarly.

To address this mechanism we reconsidered the energy change Δf per lipid induced by peptide binding put forward by Huang et al.^{12,26} For P/L > P/L*, Δf resulted in a linear decrease in the inserted peptide fraction Φ when plotted as a function of $1/(P/L)$. This is supported by oriented circular dichroism data.¹² Furthermore, several studies performed by the same group have demonstrated that Φ critically depends on the level of hydration, thus shifting P/L* to higher values if the system is partially dehydrated. Similarly, it is well known that bilayers are restricted in their spectrum of fluctuations if studied under osmotic pressure, or equivalently, at relative humidities (RH) below 100%.^{63,64} Taking all of these experimental findings into account has led us to believe that certain considerations were not previously accounted for in the original formulation of the free energy, which would affect the S–I equilibrium.^{12,26}

One of the more obvious things to consider is the entropy corresponding to the ensemble of bound peptides on the surface of which only a volume fraction Φ is inserted into the membrane. In this case, apart from the Huang¹² energy per lipid, Δf , one should also consider the lattice-gas surface entropy⁶⁵ Δs so that the total excess free energy is $\Delta f - T\Delta s$. In Huang's case, the minimization of energy change Δf per lipid gives the equilibrium condition¹² in a form that reads simply as

$$\frac{\partial \Delta f}{\partial \Phi} = 0 \quad (11)$$

leading to a functional dependence of Φ on P/L, $\Phi(P/L)$.^{12,26} Adding the surface entropy for membrane-bound peptides to the equilibrium considerations, i.e., minimizing the total free energy per lipid, $\Delta f - T\Delta s$, as opposed to just the energy term Δf , leads to a more complicated equilibrium condition that can be cast as

(60) Press, W. H.; Teukolsky, S. A.; Vetterling, W. T.; Flannery, B. P. *Numerical Recipes: The Art of Scientific Computing*, 3rd ed.; Cambridge University Press: Cambridge, U.K., 2007.

(61) McIntosh, T. J.; Simon, S. A. *Biochemistry* **1986**, *25*, 4058.

(62) Huang, H. W.; Wu, Y. *Biophys. J.* **1991**, *60*, 1079.

(63) Katsaras, J. *Biophys. J.* **1998**, *75*, 2157.

(64) Nagle, J. F.; Katsaras, J. *Phys. Rev. E* **1999**, *59*, 7018.

(65) Hill, L. T. *An Introduction to Statistical Thermodynamics*; Dover Publications: New York, 1986.

(56) Tristram-Nagle, S.; Petrache, H. I.; Nagle, J. F. *Biophys. J.* **1998**, *75*, 917.

(57) Fox, R. O., Jr.; Richards, F. M. *Nature* **1982**, *300*, 325.

(58) Svergun, D. I.; Barberato, C.; Koch, M. H. J. *J. Appl. Crystallogr.* **1995**, *28*, 768.

(59) Bak, M.; Bywater, R. P.; Hohwy, M.; Thomsen, J. K.; Adelhorst, K.; Jakobsen, H. J.; Sorensen, O. W.; Nielsen, N. C. *Biophys. J.* **2001**, *81*, 1684.

$$\Phi = \frac{1}{2} \left(1 - \tanh \frac{1}{2k_B T} \frac{\partial \Delta f}{\partial \Phi} \right) \quad (12)$$

and has a form that is standard for lattice-gas systems.⁶⁵ The derivative $\partial \Delta f / \partial \Phi$ in both of the above equations contains, as a prefactor, the numerical coefficient $K_A / (k_B T) (A_P^2 / A_L) (1 - \beta)^2$, where K_A is the area compressional modulus, $k_B T$ is the thermal energy, A_L is the cross-sectional area per lipid, A_P is defined as the lipid area increase due to one peptide in the S state, and β accounts for differential effects of peptides in the I and S states¹² and can be derived on inspection of eq 3 in ref 12. If this numerical coefficient is large enough, which simply means that the surface-energy term Δf dominates the surface entropy term $T\Delta s$, then the second equilibrium condition, eq 12, is reduced to eq 11. In simple terms, if the surface energy of bound peptides dominates their surface entropy, it then dictates the equilibrium conditions. For the most part, entropy simply softens the behavior of eq 11 as analyzed by Huang et al.¹² This smoothing effect of the entropy can also be seen in other contexts, for example, in the Poisson–Boltzmann theory of electrostatic interactions.⁶⁶ In the case of Poisson–Boltzmann theory, the electrostatic energy would lead to a sharp increase in the counterion concentration close to a charged wall, but the ideal translational entropy softens this sudden surge of counterions into a smooth exponential with a Debye–Hückel screening length!

As stated, the Huang equilibrium condition (eq 11) results in a linear decrease in the fraction of inserted peptide Φ when plotted as a function of $1/(P/L)$. A decrease in Φ is also observed if the entropy term is included in the equilibrium condition described by eq 12 (Figure 4), except that in that case Φ is smoothed out and can be fitted by an exponential function of the form $\exp(-(P/L)/(P/L)^*)$, where $(P/L)^*$ is the same as that given by Huang.¹² This is, in fact, the form that is also suggested by our experiments (Figure 3)! A plausible rationale for this result is the entropic smoothing out of the equilibrium Φ as a function of P/L . However, a direct connection of the various structural parameters to changes in Φ cannot be made because dimeric or higher oligomeric peptides deform the membrane, even in the S state.^{23,24} Furthermore, in the absence of direct measurements of Φ for fully hydrated systems, such considerations are highly speculative. Nevertheless, surface entropy evidently guides the functional behavior of the bilayer's structural parameters. By assuming this, we are also able to reconcile the lack of membrane thinning observed by Li and Salditt in certain lipid/peptide systems.³¹ If the entropy contribution is reduced, then at some point peptides will not aggregate within the bilayer to form pores and consequently will not lead to a membrane thinning effect.

Finally, we present the changes in bilayer interactions as observed by increases in d_w and η (Figure 3), which were derived from the global fits to the diffraction data (Figure 2). As noted, we took the fact that DOPC exhibits a finite bilayer separation at all alamethicin concentrations as evidence that electrostatic effects can be neglected. Hence, the only interactions that could have been affected by the presence of alamethicin are the van der Waals force, the hydration force, and/or bilayer undulations. We measured the interacting forces (i.e., equation of state) as detailed in the Materials and Methods section, with the results shown in Figure 5. Two things are apparent from the $\Pi(d_w)$ data, even in the absence of any analysis. The data differ most significantly at low osmotic pressure but basically overlap at Π

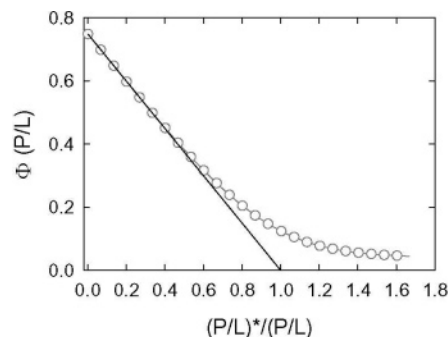


Figure 4. Numerical solutions of eq 12 with (○) and without (—) a finite surface entropy contribution, which gives rise to eq 12 as opposed to the minimization condition of eq 11. The latter coincides with the solution given by Huang,¹² which is linear in $(P/L)^*/(P/L)$ until $(P/L)^*/(P/L) = 1$, at which point it levels off to zero with a discontinuous derivative. The solution of eq 12 with surface entropy terms included is a continuous function for all values of $(P/L)^*/(P/L)$, shows no discontinuity in the derivative, and can be fit by the functional form $\exp(-(P/L)/(P/L)^*)$, which, incidentally, is also the form suggested by our experiments. We have rescaled the x axis by a constant $(P/L)^*$ defined by Huang¹² (eq 5 in ref 12). The plot is not meant to represent any measured data but merely illustrates the principle of how finite entropy terms change the dependence of Φ on P/L .

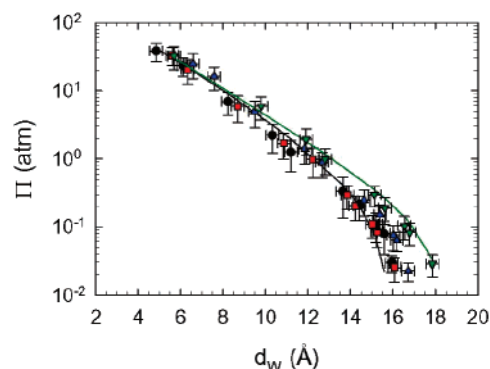


Figure 5. Equation of state for DOPC in the presence of alamethicin at 25 °C. Representation of $\Pi(d_w)$ data of pure DOPC (●), $P/L = 1/700$ (red □), $P/L = 1/200$ (blue Δ), and $P/L = 1/25$ (green ▽). The solid lines are fits to the data of pure DOPC bilayers (black line) and $P/L = 1/25$ (green line).

> 10 atm. This implies that short-range interactions, such as hydration forces, are not affected by the presence of the peptide. Only the long-range forces are modified, which in the present case are given by a balance between the van der Waals and undulation interactions. However, because the change in membrane thickness amounts to only ~ 2 Å over the entire range of peptide concentrations studied, van der Waals attractions will decrease only very slightly. Consequently, the pronounced increase in bilayer separation at low Π for high alamethicin content must be the result of increased fluctuation pressure.

To gain quantitative insight, we have analyzed the $\Pi(d_w)$ data in terms of interacting forces. As described, we first determined the parameters $P_h = 590 \pm 180$ atm and $\lambda_h = 2.1 \pm 0.1$ Å for the hydration pressure at high Π using $H = 4.3$ zJ.⁵³ Our result for λ_h agrees well with previous reports.^{50,67,68} The value of P_h depends very much on the definition of the membrane thickness, but is in agreement with previously published data.^{50,69} Deviations at low Π then have to originate from bending fluctuations. We determined the empirical scaling constant $A_{\Pi} = 0.85 \pm 0.2$ Å⁻²

(66) Andelman D. In *Soft Condensed Matter Physics in Molecular and Cell Biology*; Poon, W. C. K., Andelman, D., Eds.; CRC Press: Boca Raton, FL, 2006; p 97.

(67) Rand, R. P.; Parsegian, V. A. *Biochim. Biophys. Acta* **1989**, 988, 351.

(68) McIntosh, T. J.; Simon, S. A. *Biochemistry* **1993**, 32, 8374.

(69) McIntosh, T. J.; Magid, A. D.; Simon, S. A. *Biochemistry* **1987**, 26, 7325.

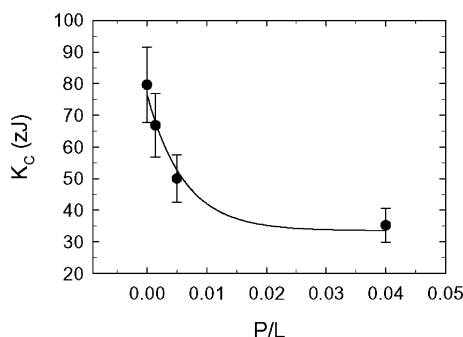


Figure 6. Bending rigidities of DOPC bilayers at 25 °C in the presence of alamethicin. The solid line indicates an exponential decay of K_C with $(P/L)^* = 160$.

by setting $\lambda_{fl} = 2\lambda_h$ and fixing K_C at 80.0 zJ.⁴⁸ Finally, we fixed A_{fl} for all four $\Pi(d_w)$ data sets at the previously determined value and left K_C and λ_h as the only adjustable parameters. Figure 6 shows the results for the bending rigidity obtained from this analysis, which is shown to drop as a function of peptide concentration, from ~ 80.0 to 35.0 zJ. The observed variation of λ_h for $P/L = 0, 1/700, 1/200,$ and $1/25$ was negligible and within the accuracy of 0.1 Å.

To check for the possible effect of a change in A_{fl} as a function of P/L , we fixed its value at 1.3 \AA^{-2} at the highest peptide concentration. This led to a slight decrease in λ_h to 1.94 Å, but to a similar value for K_C . As an additional independent check we have pursued an alternative approach similar to the one applied to DMPC near its main phase-transition temperature⁵¹ and have found K_C to decrease. Hence, our results concerning the bilayer's bending rigidity as a function of peptide concentration, are seemingly robust. It should be noted that reported K_C values usually show a large spread depending on the experimental technique used. In the case of DOPC, K_C values range from 24 to 85 zJ.⁷⁰ Nevertheless, we are more interested in the relative changes to K_C with peptide concentration, not its absolute value.

We found approximately a 2-fold reduction in the bending rigidity of DOPC as the level of alamethicin is increased up to $P/L = 1/25$ (Figure 6). Because of this drop, one would also expect a contribution to the harmonic approximation of the interaction potential in the form of the compressibility modulus B (eq 7) which consists of a bare, fluctuation-dependent interaction part.⁵⁰ Indeed, we find a drop in B by about 15% in the presence of the peptide when using the data presented in Figures 3 and 6. The decreases in K_C and B are clear evidence that the disorder induced by alamethicin not only leads to disorder within the bilayer, but also significantly affects the bilayer's mechanical properties. Moreover, K_C follows the same exponential behavior observed for $d_B, A_L, d_w,$ and η (Figure 3), as indicated by the

solid line (Figure 6). Hence the bilayer's bending rigidity is obviously coupled to membrane disorder, and follows the same mechanism discussed above. This means that alamethicin not only affects the bilayer structure, but also the membrane's elasticity. The important aspect of this finding is that the softening of the lipid bilayer, induced by the peptide, modulates the membrane-mediated interactions between the peptides. Thus, the formation of alamethicin dimers or oligomers, which are precursor states to pore formation, will most likely be facilitated when the membrane's bending rigidity is reduced. In other words, alamethicin appears to soften up the bilayer to enable it to penetrate the membrane.

4. Conclusions

We have provided experimental evidence showing that alamethicin leads to significant disorder in fully hydrated DOPC multibilayers. This disorder is manifested in the form of membrane thinning, increase to the lateral area per lipid and a decrease in the membrane's bending rigidity. We believe that softening of the lipid bilayer significantly influences lipid-mediated peptide-peptide interactions and should be included in future theoretical considerations. The observed membrane thinning was found to be in agreement with previous studies by Huang and co-workers.¹² However, our data did not exhibit a linear decrease to d_B below a certain threshold value P/L^* and a constant d_B above P/L^* . Instead, we found d_B to decrease exponentially with a decay constant close to the P/L^* value reported for DOPC/alamethicin.⁶² Furthermore, this exponential behavior, with the same P/L^* value, was found for all of the other structural parameters, including that of the bending rigidity. This was understood by considering entropic contributions previously neglected in the free-energy description of the $S \rightarrow I$ transition.^{12,26} Importantly, this also resolves the apparent disagreement in the observed membrane thinning effect^{12,31} because a decrease in the entropy term, due to lower levels of hydration, leads to a sharpening of the transition point and a shift to higher P/L^* values. Given the large number of parameters relating to properties of individual lipid and peptide molecules, it is not surprising that we have not been able to cast our findings into a more general picture of lipid/peptide interactions. Moreover, we also cannot rule out membrane thickening as taking place in certain lipid/peptide systems.³¹ Nevertheless, our study has clearly emphasized the importance of entropy, which needs to be considered in future lipid/peptide interaction studies of model systems.

Acknowledgment. We thank Karin Ovari for assistance in performing dilatometric experiments and Karl Lohner for several helpful discussions. This work has been supported by the Austrian Science Fund FWF (grant no. P17112-B10 to G.P.).

(70) Rappolt M.; Pabst, G. In *Structure and Dynamics of Membrane Interfaces*; Nag, K., Ed.; Wiley: New York; in press, 2007.